



International Institute for  
Applied Systems Analysis  
Schlossplatz 1  
A-2361 Laxenburg, Austria

Tel: +43 2236 807 342  
Fax: +43 2236 71313  
E-mail: [publications@iiasa.ac.at](mailto:publications@iiasa.ac.at)  
Web: [www.iiasa.ac.at](http://www.iiasa.ac.at)

---

## **Interim Report**

**IR-06-076**

### **The wave speed of intergradation zone in two-species lattice Müllerian mimicry model**

Isao Kawaguchi ([kawag@nirs.go.jp](mailto:kawag@nirs.go.jp))

Akira Sasaki ([asasascb@mbox.nc.kyushu-u.ac.jp](mailto:asasascb@mbox.nc.kyushu-u.ac.jp))

---

#### **Approved by**

Ulf Dieckmann

Program Leader, Evolution and Ecology Program

December 2006

---

*Interim Reports* on work of the International Institute for Applied Systems Analysis receive only limited review. Views or opinions expressed herein do not necessarily represent those of the Institute, its National Member Organizations, or other organizations supporting the work.

## Contents

Abstract.....	3
Introduction .....	4
Model.....	6
Results .....	11
Discussion.....	16
Acknowledgement.....	20
Appendix A .....	21
Appendix B.....	23
Literature Cited.....	24
Figure Legend.....	26
Figures .....	29

# The wave speed of intergradation zone in two-species lattice Müllerian mimicry model

Isao Kawaguchi<sup>1\*</sup> and Akira Sasaki<sup>2,3</sup>

<sup>1</sup>Regulatory Sciences Research Group, Research Center for Radiation Protection,  
National Institute of Radiological Sciences, Chiba, 263-8555, Japan

<sup>2</sup>Department of Biology, Faculty of Science, Kyushu University, Fukuoka 812-8581,  
Japan

<sup>3</sup>Evolution and Ecology Program, International Institute for Applied Systems Analysis,  
Schlossplatz 1, A-2361 Laxenburg, Austria

\* corresponding author:

tel: +81-43-206-3150

fax:+81-43-251-4853

Email: kawag@nirs.go.jp

Keywords: Müllerian mimicry, mimicry ring, lattice model, spatial mosaic, pair-edge  
approximation



## Abstract

A spatially explicit model is studied to analyze the movement of coupled clines in two-species a Müllerian mimicry system as exemplified by the comimicking heliconiine butterflies in Central-South America *Heliconius erato* and *H. melpomene*. In this system, a pair of comimicking wing patterns of two species (mimicry ring) is found in a geographical region but another pair of wing patterns is found in a different geographical region. The distribution of mimicry rings thus form a spatial mosaic in a large geographical scale, and the mechanism responsible for their stable maintenance has been a long standing question in evolutionary biology. We here examine the speed of the movement of boundaries that divide the regions inhabited by different mimetic morphs in each comimicking species, by assuming coupled two-state stochastic cellular automata where the flipping rate of the site occupied by a mimetic morph depends on the local density of the same morph and of the comimicking morph in the other species. The speed of cline movement shows a complex dependence on the coupling parameter between mimetic species -- greater coupling of comimicking morphs between species slows down the cline movement only when the reduction in predation rate exhibits diminishing return to the increase of local mimetic morph density. The analytical predictions are confirmed by the results of Monte Carlo simulations. The speed of advance is quite different from that predicted from the conventional reaction-diffusion model, indicating that demographic stochasticity plays a critical role in determining the speed of cline movement. We also examine if the spatial heterogeneity in migration rate can stably maintain clines.

## **Introduction**

Müllerian mimicry stands for the comimicry of unpalatable species in their warning coloration (e.g. wing patterns). If the wing pattern of two or more species resemble with each other in a local population, the predation rate should be more effectively reduced because a predator learns their unpalatability more quickly. This will increase the frequency of the comimicking morph in each species, which finally will establish itself in a local geographical region. Sibling species of the tropical butterflies, *Heliconius erato* and *H. melepomene* is one of the best known examples of Müllerian mimicry, in which many different kinds of locally comimicking morphs are distributed over Central-South America, forming a patchwork of mimicry rings (a mimicry ring is defined as a set of species with comimicking warning coloration) in a large geographical scale with sharp boundaries (intergradation zones) dividing them.

This well known example, which has clearly demonstrated the power of natural selection in phenotypic evolution, has also been one of the most serious challenges from nature to theoretical evolutionary biology. The problem is why does not the spatial mosaic of mimicry rings coalesce into a single comimicking pattern. If one morph enjoys a selective advantage over the other, due to for example the difference in the brightness of wing patterns which would in turn affect the propensity to be found by predators, the advantageous morph should gradually expand its range of distribution and finally replace the other. It therefore remains a mystery why so many mimetic morphs are stably maintained as a spatial mosaic, because it is hardly believable that morphs suffer exactly the same predation pressure at the boundary. This is the problem we examine in this paper --- we will not pursue another puzzle in Müllerian mimicry, the coexistence of Müllerian mimicry rings in one geographical area (Mallet and Joron 1999) .

Various hypotheses have been proposed so far for the factor responsible for the maintenance of the spatial mosaic in Müllerian mimicry system (Barton 1979; Barton and Hewitt 1989; Brown and Benson 1974; Mallet et al. 1990; Mallet and Turner 1998; Sasaki et al. 2002), but very few has taken into account demographic stochasticity which would largely affect the process (but see Barton 1979). Recent theoretical studies (Ellner et al. 1998, Kawasaki et al. 2006) show that a striking difference exists in the speeds of propagation of a single species in spatially explicit model (lattice model or stochastic cellular automata model) and that of reaction diffusion models which discard any kind of stochasticity.

Here we study an individual-based model that describes the demographic process of two species and examine the speed at which the boundary for different pairs of comimicking morphs move in each species. Individuals of each species are assumed to be distributed on a linear lattice, and the site open by mortality of an individual will be immediately colonized by one of the nearest neighbors of the same species. The mortality of an individual is assumed to decrease with the number of nearest neighbor sites occupied by individuals of the same wing pattern and that of the comimicking wing pattern in the other species. This is therefore a spatially explicit analogue of the reaction-diffusion models for the spread of alleles under frequency-dependent selection favoring a commoner type. Our model incorporates two additional factors, demographic stochasticity and the interaction between two species, that have been ignored in previous models. By constructing a Markov chain model describing the change in the distance between the mimetic-morph-boundaries of each species, analytical results for the speeds of cline movement in two species will be derived. We then ask how these additional factors, demographic stochasticity and interspecific interaction, affect the speed of the movement of intergradation boundary and the conditions for the maintenance of spatial mosaic. Analytical results will be compared to those of extensive Monte Carlo simulations. We then analyze the speed of propagation in a two

dimensional habitat, and the effect of spatially heterogeneity in population structure in maintaining the spatial mosaic.

## Model

We consider two comimicking butterfly species in a one dimensional lattice space, and assume that there are two mimetic morphs  $A$  and  $B$  in species 1,  $a$  and  $b$  in species 2. The morphs  $A$  and  $a$  are a comimicking pair of warning coloration (a mimicry ring), and  $B$  and  $b$  are another comimicking pair (mimicry ring). It is convenient to consider two lattices in parallel (dual lattice), each describes the spatial configuration of mimetic morph of one mutually interacting species. Each site in a lattice open by the mortality of an individual is assumed to be immediately filled by the progeny sent by one of the nearest neighbors of the same species. We denote by  $N_A(x)$  the number of individuals with morph  $A$  in the neighborhood of site  $x$ , i.e., the number of  $A$ 's found in the sites  $x-1$ ,  $x$ , and  $x+1$ . We drop the argument  $x$  for notational simplicity whenever the meaning is clear. The quantities  $N_B$  of the same species, and  $N_a$ , and  $N_b$  of the other species are defined similarly.

We assume that the mortality  $d_A$  of an individual with mimetic morph  $A$  depends both on the number  $N_A$  of conspecific individuals having morph  $A$  in the neighborhood of the site at census, and on the number  $N_a$  of individuals with the comimicking morph  $a$  of the other specie. Specifically, we assume that the effect of the comimicking morph of the other species is to reduce the predation rate of morph  $A$  individual by the amount equivalent to increase the morph  $A$  density to:  $N_A \rightarrow N_A + \sigma N_a$ , where  $\sigma$  is a positive constant between 0 and 1. We call  $N_A + \sigma N_a$  the effective local density of morph  $A$ . The parameter  $\sigma$  describes the similarity between comimicking pair of morphs  $A$  and  $a$ , and between  $B$  and  $b$ , where  $\sigma = 0$  implies that there is no similarity between "comimicking" pair of morphs (and hence they are not comimicking at all); whereas,  $\sigma = 1$  implies perfect comimicry with which the predator cannot distinguish the

difference between species if they have comimicking morphs. The mortality of each morph is then given by

$$\begin{aligned}
 d_A(N_A + \sigma N_a) &= u_0 + u_1 \varphi_A(N_A + \sigma N_a), \\
 d_B(N_B + \sigma N_b) &= u_0 + u_1 \varphi_B(N_B + \sigma N_b), \\
 d_a(N_a + \sigma N_A) &= u_0 + u_1 \varphi_A(N_a + \sigma N_A), \\
 d_b(N_b + \sigma N_B) &= u_0 + u_1 \varphi_B(N_b + \sigma N_B),
 \end{aligned} \tag{1}$$

where  $u_0$  denotes base mortality (the mortality not due to predation),  $u_1$  is the maximum mortality by predation which is attained, for the case of  $d_A$  and  $d_a$ , when local populations of morph  $A$  and  $a$  approach zero. The functions  $\varphi_A(N)$  common to the comimicking pair  $A$  and  $a$ , and  $\varphi_B(N)$  common to the comimicking pair  $B$  and  $b$  describe how the predation rate depends on the local density  $N$  of the same morph and the comimicking morph in the neighborhood

$$\begin{aligned}
 \varphi_A(N) &= \frac{1}{1 + e^{\delta(N - \alpha_A)}}, \\
 \varphi_B(N) &= \frac{1}{1 + e^{\delta(N - \alpha_B)}}.
 \end{aligned} \tag{2}$$

Both  $\varphi_A$  and  $\varphi_B$  are sigmoidally decaying function of  $N$ , differing only in their inflection points  $\alpha_A$  and  $\alpha_B$ . The parameter  $\delta$  is a positive constant describing the strength of density dependence in predation rate (and hence measuring the intensity of frequency-dependent selection favoring a commoner morph). Positive constants  $\alpha$ 's give the half-mortality densities, the density at which the mortality due to predation is halved from its maximum, and also at which the sensitivity to density is the largest. A larger  $\alpha$  indicates that more density is required to reduce the predation rate to a given level. For example, a dull colored morph might require larger number of captures to make the predator efficiently learn its unpalatability than a bright colored morph. Throughout the paper, we assume that the comimicking pair of morphs  $A$  and  $a$  is advantageous over the other comimicking pair of morphs  $B$  and  $b$ , by assuming that

$\alpha_A \leq \alpha_B$ . By this assumption, the mortality of comimicking morphs  $B$  and  $b$  for a given effective local density is always larger than that of the pair  $A$  and  $a$  with the same effective local density.

An example of spatial configuration of mimetic morph distribution in each species, and their mortality at each sites are illustrated in Figure 1. In this figure and thereafter we assume that comimicking pair  $A$  and  $a$  are distributed to the left of boundaries and  $B$  and  $b$  to the right. By assumption the configuration may change if and only if one of the individuals next to the boundary dies, because the open site in the midst of the cluster will be filled by the same morph. We are interested in the movements of  $A$ - $B$  boundary in species 1 and  $a$ - $b$  boundary in species 2. We call the right most individual of  $A$ -cluster and the left most individual of  $B$ -cluster the 'front-runners' (Ellner et al. 1998). The front runners of species 2 are defined in the same vein. The position of  $A$ - $B$  boundary of species 1 move one step right when morph  $B$  front runner dies and the open site is filled by the progeny of morph  $A$  front runner. The probability that this event occurs in a unit time interval is therefore  $d_B(2 + \sigma N_b) \times (1/2)$ , in which  $d_B(2 + \sigma N_b)$  is the mortality of the morph  $B$  front runner which should have had 2 conspecific individuals of the same morph in the neighborhood and  $N_b$  individuals, which depends on the position of  $a$ - $b$  boundary of species 2, of comimicking morph of the other species in the same neighborhood. This is then multiplied by  $1/2$ , the probability that the open site is occupied by the progeny from the left. Similarly, the rate at which the  $A$ - $B$  boundary moves one-step left is  $d_A(2 + \sigma N_a) \times (1/2)$ . The speed  $v$  of the movement of  $A$ - $B$  boundary is therefore given by

$$v = \frac{u_1}{2} E[\varphi_B(2 + \sigma N_b) - \varphi_A(2 + \sigma N_a)], \quad (3)$$

where we use (1). We will show below that the speed of the movement of  $a$ - $b$  boundary is the same as that of  $A$ - $B$  boundary if the distance between the boundaries has a

stationary probability distribution, and that this is the case in our model.  $E[\cdot]$  in (3) denotes taking expectation over possible local densities of comimicking morphs in the other species in the neighborhood of front runners, which is equivalent to take expectations over the distance  $d$  between  $A$ - $B$  boundary and  $a$ - $b$  boundary because the local densities of comimicking morphs in the neighborhood of front runners are uniquely determined by specifying  $d$ . To get the speeds, it is then suffice to obtain the probability distribution for the distance  $d$  between mimetic morph boundaries of two species.

Let us define  $p_d(t)$  as the probability at time  $t$  that  $A$ -front runner in species 1 is  $d$  step ahead of the  $a$ -front-runner in species 2, which then obey a birth-death process:

$$\dot{p}_d = \mu_{d+1}p_{d+1} + \lambda_{d-1}p_{d-1} - \mu_d p_d - \lambda_d p_d, \quad (d = 0, \pm 1, \pm 2, \dots) \quad (4)$$

where  $\lambda_d$  is the transition rate from  $d$  to  $d+1$ , and  $\mu_d$  is the transition rate from  $d$  to  $d-1$ , which will be specified below. There are two ways by which the distance change from  $d$  to  $d+1$  -- one is that the  $A$  front-runner moves a step forward in species 1, and the other is that the  $a$  front runner moves a step backward in species 2. This and similar consideration for the transition from  $d$  to  $d-1$  yield the transition rates  $\lambda_d$ 's and  $\mu_d$ 's:

$$\left\{ \begin{array}{l} \lambda_d = \mu_{-d} = \frac{1}{2}(d_A(2+3\sigma) + d_B(2+3\sigma)), (d \geq 1) \\ \lambda_0 = \mu_0 = \frac{1}{2}(d_A(2+2\sigma) + d_B(2+2\sigma)), \\ \lambda_{-1} = \mu_1 = \frac{1}{2}(d_A(2+\sigma) + d_B(2+\sigma)), \\ \lambda_d = \mu_{-d} = \frac{1}{2}(d_A(2) + d_B(2)), (d \leq -2) \end{array} \right. \quad (5)$$

or using (1),

$$\lambda_d = \mu_{-d} = u_0 + u_1 \left\{ \begin{array}{l} [\varphi_A(2+3\sigma) + \varphi_B(2+3\sigma)]/2, \quad (d \geq 1) \\ [\varphi_A(2+2\sigma) + \varphi_B(2+2\sigma)]/2, \quad (d = 0) \\ [\varphi_A(2+\sigma) + \varphi_B(2+\sigma)]/2, \quad (d = -1) \\ [\varphi_A(2) + \varphi_B(2)]/2, \quad (d \leq -2) \end{array} \right. \quad (6)$$

In Appendix A, we derive the stationary probability density  $\hat{p}_d$  of the process:

$$\begin{aligned}\hat{p}_d &= \hat{p}_{-d} = \hat{p}_0 \theta_1 \theta_2^{d-1}, & (d=1,2,\dots), \\ \hat{p}_0 &= 1/[1+2\theta_1(1-\theta_2)^{-1}],\end{aligned}\tag{7}$$

with

$$\theta_1 = \frac{\lambda_0}{\mu_1} \quad \text{and} \quad \theta_2 = \frac{\lambda_1}{\mu_2}.$$

The stationary distribution for the distance  $d$  between boundaries is symmetric around  $d=0$ , and both tails decay geometrically with the factor  $\theta_2$ . Since  $\theta_2 < 1$  always holds for  $\sigma > 0$ , the stationary distribution (7) is well-defined. If on the other hand  $\sigma = 0$ , the mimetic morph boundaries of two species move independently, as one should expect. Using this, the speed of the movement of boundary (3) becomes

$$v = \frac{u_1}{2} \left( \sum_{d=-\infty}^{\infty} \varphi_B(n_B(d)) \hat{p}_d - \sum_{d=-\infty}^{\infty} \varphi_A(n_A(d)) \hat{p}_d \right),\tag{8}$$

where  $n_A(d)$  and  $n_B(d)$  respectively denotes the local density experienced by the morph A front-runner and the morph B front-runner when A-B boundary of species 1 is  $d$  step ahead of a-b boundary of species 2. Note that for a front runner at the site  $x$  there are 2 conspecific individuals in the neighborhood of  $x$  (the sites  $x-1$ ,  $x$ , and  $x$ ) having the same wing pattern as the front runner. We then see, by counting the number of  $a$ -individuals in the neighborhood of the front runner of A's for a given distance  $d$  to the  $a$ - $b$  boundary, that  $n_A(d) = 2 + 3\sigma$  for  $d \leq -1$ ;  $n_A(0) = 2 + 2\sigma$ ;  $n_A(1) = 2 + \sigma$ ; and  $n_A(d) = 2$  for  $d \geq 2$ . Because of the symmetry  $n_A(d) = n_B(-d)$  follows for all  $d$ . By exchanging  $d$  and  $-d$  in the first term of RHS of (8), and using  $\hat{p}_d = \hat{p}_{-d}$  and  $n_A(d) = n_B(-d)$ , the formula for the wave speed (8) can be rewritten as

$$v = \frac{u_1}{2} \sum_{d=-\infty}^{\infty} [\varphi_B(n_A(d)) - \varphi_A(n_A(d))] \hat{p}_d,$$

or by substituting  $n_A(d)$ 's,

$$v = \frac{u_1}{2} \left[ (\varphi_B(2) - \varphi_A(2)) \sum_{d=2}^{\infty} \hat{p}_d + (\varphi_B(2 + \sigma) - \varphi_A(2 + \sigma)) \hat{p}_1 \right. \\ \left. (\varphi_B(2 + 2\sigma) - \varphi_A(2 + 2\sigma)) \hat{p}_0 + (\varphi_B(2 + 3\sigma) - \varphi_A(2 + 3\sigma)) \sum_{d=1}^{\infty} \hat{p}_d \right] \quad (9)$$

Thus the wave speed is expressed as the weighted average of the inter-morph difference in predation rates when their front runners are in the same condition as to the number of comimicking morphs in the neighborhood. The terms including the sum of stationary probability distribution are evaluated from (7) as

$$\sum_{d=1}^{\infty} \hat{p}_d = \frac{1 - \hat{p}_0}{2}, \quad \sum_{d=2}^{\infty} \hat{p}_d = \frac{1 - \hat{p}_0}{2} - \theta_1 \hat{p}_0. \quad (10)$$

With this and  $\hat{p}_0$  and  $\hat{p}_1$  defined in (7), we obtain that the speed  $v$  defined in (9) as a function of parameters,  $u_1$ ,  $\sigma$ ,  $\alpha_A$ ,  $\alpha_B$ , and  $\delta$  (the speed is independent of the base mortality  $u_0$ ).

## Results

The joint speed of the movement of mimetic morph boundaries obtained from (7), (9), and (10) is illustrated in Fig. 2 as a function of  $\sigma$ , the similarity between comimicking pair of morphs, and is compared with the results of Monte Carlo simulation. The predicted results fit very well to the simulated ones. The speed decreases as the similarity  $\sigma$  increases toward 1 (where the comimicry is perfect). This result seems to have a clear biological meaning -- the front runners that step into the kingdom of the other comimicking pair of warning coloration should then suffer a higher mortality than the conspecific individual whose warning coloration matches that of the other species. One may think that this should reduce the joint speed of the movement of mimetic morph boundaries in two species system from that in the single species system, which corresponds to the speed at  $\sigma = 0$ . In the following we will show

that this interpretation is wrong, and will show that the wave speed is primarily determined by the sensitivity of the predation rate to the morph density at the intergradation zone, and hence increasing  $\sigma$  can either speed up or slow down the wave speed, depending on whether the morph density at the intergradation zone is above or below the inflection point of density dependent predation rate. Moreover, if the predation rate is a linear function of the density, the wave speed is independent of  $\sigma$  – adding comimicking species does not change the wave speed at all.

Figure 3 illustrates such counter-intuitive dependence of the wave speed on the coupling parameter  $\sigma$ . Clearly from Fig. 3, the wave speed is not in general a monotonically decreasing function of  $\sigma$  – it can have a hump at an intermediate  $\sigma$ , or even monotonically increasing with  $\sigma$ . To see this more closely, we examine below how the wave speed depends on  $\sigma$  and the other parameters for some analytically tractable limiting cases.

When the wave fronts of two species are found in the same location most of the time (i.e,  $\hat{p}_0$  is close to 1 when  $u_0$  and  $e^{-\delta\sigma}$  are sufficiently small), the formula (9) for the speed is greatly simplified. In the limit of  $\hat{p}_0 \rightarrow 1$ , the wave speed reduces to

$$v \rightarrow \frac{1}{2}u_1\varphi_B(2+2\sigma) - \frac{1}{2}u_1\varphi_A(2+2\sigma), \quad (\hat{p}_0 \rightarrow 1). \quad (11)$$

If we further assume that the advantage of comimicking pair  $A$  and  $a$  over that of  $B$  and  $b$  is small,  $\beta = \alpha_B - \alpha_A \ll 1$ , we can expand (11) in a Taylor series with respect to  $\beta$  to have an approximate speed:

$$v \approx \frac{1}{2}u_1\varphi_0(1-\varphi_0)\delta\beta, \quad (\hat{p}_0 \approx 1 \text{ and } \beta \ll 1), \quad (12)$$

where  $\varphi_0 = \varphi_B(2+2\sigma) = 1 / (1 + e^{\delta(2+2\sigma-\alpha_B)})$ . Thus the approximate wave speed is a quadratic function of  $\varphi_0$ , and hence has a maximum at  $\varphi_0 = \varphi_B(2+2\sigma) = 1/2$ , or at  $\sigma^* = \alpha_B / 2 - 1$  (see (2) with  $N=2+2\sigma$ ). Therefore if  $\sigma^*$  lies in the range between 0 and 1, i.e. if  $2 < \alpha_B < 4$ , the wave speed first increases by increasing  $\sigma$ , attains the

maximum at  $\sigma = \alpha_B / 2 - 1$ , and decreases as  $\sigma$  approaches 1. If  $\alpha_B \leq 2$ , the wave speed is monotonically decreasing with  $\sigma$ . Conversely and the most counter-intuitively, the wave speed is monotonically increasing with  $\sigma$  when  $\alpha_B \geq 4$  -- the presence of comimicking species will speed up the movement of boundary between mimicry rings! The argument based on the approximate speed (12) agrees well with the exact speed obtained from (7), (9) and (10), as long as the parameters are to give  $\hat{p}_0 \approx 1$  and small  $\beta$  (see Fig. 3).

These results are due to the nonlinearity in density-dependent predation rates  $\varphi_A$  and  $\varphi_B$ . As is seen in the wave speed formula (8), the wave speed can be expressed as the weighted average (weighted by the stationary probability distribution for the interspecific distance in morph boundaries) of the difference in the mortalities between front runners of morph *A* and *B*. The larger is the mortality difference between *A* front runner and *B* front runner at corresponding configuration, the larger is the wave speed. Therefore if the inflection densities  $\alpha_A$  and  $\alpha_B$  are as large as the typical local densities experienced by the front runners (e.g. at  $2+2\sigma$ ), the inter-morph difference is the most magnified, and the speed is the largest. Similarly, if the inflection densities  $\alpha_A$  and  $\alpha_B$  are much larger than the local densities experience by front runners, increasing  $\sigma$  will amplify the mortality difference between morphs, and will increase the speed. “Intuitively count” results are expected only when the inflection densities  $\alpha_A$  and  $\alpha_B$  are low.

To show the importance of the sensitivity in nonlinear predation rate more clearly, we consider the case where the predation rates linearly depend on the densities. In this case, as is clear from (9), all dependence on  $\sigma$  will be canceled out, and hence the wave speed is independent of  $\sigma$  (see the dashed line in Fig 3).

The influence of the selection intensity parameter  $\delta$  on the wave speed shows a similar twist. If either  $\delta$  is too small or too large, all the transition rates approach the same value ( $\lambda_d = \mu_{-d} \approx u_0$  for small  $\delta$  or  $\lambda_d = \mu_{-d} \approx u_0 + u_1 / 2$  for large  $\delta$ ). Therefore,

the inter-morph difference in the mortalities of front runners becomes very small, resulting in a slow wave speed. The wave speed is maximized at an intermediate selection intensity  $\delta$ .

Although not important in determining the wave speed, the effect of positive  $\sigma$  in increasing the mortality of front-runners jutting out into the region where the other comimicking pair of morphs predominate, is important in manifesting the mimetic morph boundaries of two species coalesce into the same geographical region. This can be seen by the variance in the distance  $d$  between two boundaries, which will be evaluated using the stationary distribution (7) as

$$\text{Var}(d) = \sum_{d=-\infty}^{\infty} d^2 \hat{p}_d - \left( \sum_{d=-\infty}^{\infty} d \hat{p}_d \right)^2 = \frac{2\theta_1(1+\theta_2)}{(1-\theta_2+2\theta_1)(1-\theta_2)^2}, \quad (13)$$

Figure 4 illustrates how the variance depends on  $\theta_1$  and  $\theta_2$ . The variance in  $d$  most sensitively increases as  $\theta_2$  approaches 1, i.e., when the decay rate in  $\hat{p}_d$  approaches zero. By increasing the coupling parameter  $\sigma$ ,  $\theta_2$  decreases and the mimetic morph boundaries of two species become more tightly attracted with each other.

#### HETEROGENEITY IN MIGRATION RATE AND THE MAINTENANCE OF MOSAIC

Above analyses concentrated under what conditions the speed of the expansion of advantageous mimetic morph can be reduced. However, none of the factors including strong two species interaction can completely stop the movement of boundaries. In an accompanying paper on the interfacial dynamics theory of reaction-diffusion model for Müllerian mimicry rings (Sasaki et al. 2002), it is shown that the stable cline can be maintained under the interplay between spatial heterogeneity in base fitnesses, negative curvature of clines in two dimensional habitat, and the sectors of low population density and dispersal (Barton 1979; Barton and Hewitt 1989; Bazykin 1969; Sasaki et al. 2002). A practically interesting question is that if these results remain true in spatially explicit models where the selection-driven processes are largely perturbed by demographic

stochasticity. We here introduce one of such spatial heterogeneities in population structure, the sector of low migration rates, into the model, and examine whether it can stably maintain cline in a single species Müllerian mimicry system.

As before we assume that individuals with either of two mimetic morphs  $A$  and  $B$  are distributed over one dimensional lattice. Suppose that initially the sites left to a boundary are occupied by morph  $A$  individuals and those right to the boundary by morph  $B$ , and call the right most individual of morph  $A$  the front runner. Let  $q_x(t)$  be the probability at time  $t$  that the front-runner is found at the site  $x$ . We assume that the efficiency in sending progeny to the nearest neighbors, or the fecundity at the site may vary from site to site, and denote the relative migration rate (or fecundity) at site  $x$  by  $m_x$ . This simply means that if the site at  $x$  is open by mortality, it will be filled by the progeny from left with the probability  $m_{x-1}/(m_{x-1} + m_{x+1})$ , and by the progeny from right with the probability  $m_{x+1}/(m_{x-1} + m_{x+1})$ . The other processes are the same as before except that we only consider a single species. The front-runner moves one step ahead when adjacent morph  $B$  dies (the rate of which is  $d_B(2)$ ), and is occupied by the progeny sent from the morph  $A$  front-runner at site  $x$ ; it moves one step back when morph  $A$  front runner dies (whose rate is  $d_A(2)$ ) and the site is colonized from the morph  $B$  at the site  $x+1$ . Consequently, the change in  $q_x$ 's are given by

$$\frac{dq_x}{dt} = \mu_{x+1}q_{x+1} + \lambda_{x-1}q_{x-1} - \mu_x q_x - \lambda_x q_x, \quad (14)$$

where  $\lambda_x$  and  $\mu_x$  are the transition probabilities from  $x$  to  $x+1$  and  $x$  to  $x-1$ :

$$\lambda_x = \frac{m_x}{m_x + m_{x+2}} d_B(2), \quad \mu_x = \frac{m_{x+1}}{m_{x-1} + m_{x+1}} d_A(2). \quad (15)$$

The stationary distribution  $\hat{q}_x$  for the position  $x$  of the front runner must satisfy, if it exists,

$$\hat{q}_x = \frac{1}{m_{x+1}m_x} \left( \frac{d_B(2)}{d_A(2)} \right)^x \left( \sum_{m_{y+1}m_y} \frac{1}{m_{y+1}m_y} \left( \frac{d_B(2)}{d_A(2)} \right)^y \right)^{-1}, \quad (16)$$

where sum is over all  $y$  (see Appendix B for the derivation).

As an example of the sector of low migration rates, we assume that the migration rate has a minimum at  $x=0$  and rapidly piles up as  $|x|$  increases:

$$m_x = e^{ax^2}, \quad (17)$$

where  $a$  is a positive constant. With this migration rate heterogeneity, there is a stationary distribution

$$\hat{q}_x = A e^{-2a(x-b)^2}, \quad (18)$$

where  $b = (\log d_B(2) - \log d_A(2) - 2a) / 4a$ , and  $A = \left( \sum_{x=-\infty}^{\infty} e^{-2a(x-b)^2} \right)^{-1}$ . The stationary distribution (18) is a normal distribution with mean  $x=b$ , i.e., the  $A$ - $B$  boundary is trapped around  $x=b$  with Gaussian temporal deviation. The long term average distribution for the positions of boundary observed in Monte Carlo simulation fit very well to the predicted normal distribution (18) with mean  $b$  (Fig. 5). In the simulation, the migration rate function is truncated at a maximum value and hence is bounded above. Therefore the boundary should finally get out of the valley of low migration rates, and (18) actually gives an approximate sojourn time distribution until the boundary will exit. The mean exit time should primarily depend on the depth of valley, and it is also interesting to ask how much depth is needed for the valley to trap the cline for a sufficiently long time. This is however not pursued in this paper.

## Discussion

We have analyzed the movement of clines in a two species Müllerian mimicry system by deriving a formula for the joint wave speed in a spatially explicit model on one dimensional lattice. Demographic stochasticity and two species interaction in

nonlinear density dependent selection are the factors which are ignored in the previous models and hence we focus in this paper. By evaluating the speed of the front runner by constructing a Markov process for the distance between mimetic morph boundaries in two species we have revealed a number of results which are not expected under the conventional reaction-diffusion model.

*What is the main factor to slow down the cline movement?*

The most counter-intuitive result of our model is that the increase in the interspecific interaction  $\sigma$  between comimicking morphs does not necessarily slow down the speed of cline movement. Thus the-nail-that-sticks-out-will-be-hammered-down mechanism is not the primarily important determinant of the wave speed. The "hammer" mechanism is suggested as in the following example: When the boundaries between morphs perfectly match between species (i.e., if  $d=0$ ), the front-runners  $A^*$  and  $B^*$  of morph  $A$ 's and morph  $B$ 's have equal numbers of the same and the comimicking morphs in the neighborhood ( $n_A(0) = n_B(0) = 2 + 2\sigma$ ). If in contrast the front runner of  $A$  morphs is one step ahead the front-runner of comimicking  $a$  morphs in the other species (i.e., if  $d=1$ ), the front runner  $A^*$  suffers a higher mortality than  $B^*$ , because  $A^*$  finds fewer comimicking individuals in the neighborhood than  $B^*$  ( $n_A(1) = 2 + \sigma$  and  $n_B(1) = 2 + 3\sigma$ ). This implies that the larger is  $\sigma$ , the more likely is the stepped-out front runner to retreat back to the perfectly matched position ( $d=0$ ). However, once  $A^*$  steps out, the probability that the front runner  $a^*$  of comimicking morph follows it is increased when  $\sigma$  is increased, by the same amount as the rate of pulling back the stepped-out front runner is increased. This explains why the "hammer" mechanism by increasing  $\sigma$  does not directly contribute to decrease the wave speed, and also does why the same mechanism is effective to make the probability mass of the interspecific distance between morph boundaries pile up more sharply at the perfectly matched position.

The speed is therefore determined by the difference in mortality when two morphs at the edges find the same number of comimicking morphs in the neighborhood. The speed is the fastest when the inter-morph difference in mortality experienced by front runners is the largest, and hence is the fastest when the morph density at the boundary is at the inflection point of nonlinear density-dependence in predation rate.

#### *Extension to two dimension*

Preliminary simulation study of the extension of our model to 2 dimensional lattice reveals that the surface of the cline is more smooth than that observed in two dimensional wave of the advance in a simple contact process (Ellner et al. 1998, Kawasaki et al. 2006), in which the ragged shape of the front significantly increases the wave speed in a two dimensional habitat from that in one dimensional habitat. Nevertheless, the speeds of the cline movement of Müllerian mimicry system in two dimensional model (data not shown) were higher than the ones observed in one dimensional model examined in this paper, thus agreeing with the previous results (Ellner et al. 1998, Kawasaki et al. 2006).

#### *Why do so many mimicry rings coexists in Central-South America?*

We here discuss why so many mimicry rings have been maintained in heliconiine butterflies. A number of hypotheses are proposed so far (Joron and Mallet 1998; Mallet and Gilbert 1995; Mallet and Turner 1998; Turner 1981; Turner 1984). The most straightforward hypothesis is that the spatial mosaic structure found in the geographical distribution of different mimicry rings is simply a reflection of independent coevolutionary events that have occurred in each isolated habitat presumably formed in the last glacial period. This however is not consistent with the fact that *Heliconius* genes other than those responsible for color patterns are not geographically differentiated – they are continuously distributed across the sharp intergradation zone between different mimicry rings (Gilbert 1983; Turner 1981). This

observation suggest that the butterfly can migrate over major geographical regions and their genes intermixed. It is therefore natural selection that maintain the clines and the spatial mosaic of mimicry rings. Our model revealed the conditions under which the movement of clines is significantly slowed down, but no process can completely stop the movement in a uniform habitat. We therefore need to consider some spatial heterogeneity in population structure (Barton 1979; Barton and Hewitt 1989; Bazykin 1969; Sasaki et al. 2002) to account for the stable maintenance of cline. We here extended the applicability of one of such mechanism (the clines trapped at the sector of low migration rate) to the situation where demographic stochasticity largely perturbs the process, by showing that a stationary distribution for the position of cline exists for a sufficiently deep migration trough.

Recent empirical studies show the evidence for the movement of the cline of mimetic morph and hybrid zone across apparent physical barrier. The cline of the mimetic morph of *H. erato* in Panama moves 2 km/year to westward, in spite of that lakes in the cline might have acted as partial barrier for the migration and population density; whereas, the cline of corresponding mimetic races in *H. melpomenes* did not move in the same area (Blum 2002). Interestingly, the hybrid zone of non-mimetic butterflies, *Anartia fatima* and *A. amathea*, moves toward the opposite direction but with roughly the same speed as that of *H. erato* (Dasmahapara et al. 2002).

One tends to assume that the sector of unfavorable physical environment act as an obstacle to cline movement. This is true because population density is to be decreased at the sector of unfavorable habitats, and the trough of population density can indeed trap the cline if the density trough is deep enough (Bazykin 1969, Barton 1979, Sasaki et al. 2002). However, it should be noted that if an individual tends to leave an unfavorable patch more readily than a favorable patch, the mobility of individuals at the trough might be higher than the surrounding place, which might make the effective migration across the barrier high (Mallet 1993). On the other hand, the colonization rate

to the unfavorable patch must definitely be low. Net effect of geographical barrier on the effective migration rate, on the population density, and on the force of cline trapping must therefore be analyzed in more explicit model taking into account all these factors before we can reach a final consensus.

We have assumed a symmetric interaction between two mutually comimicking species. However there is a large difference in the roles in the mimicry interaction of the two heliconiine species. *H. erato* is relatively more abundant than *H. melpomene* (Mallet 2001), and hence *H. melpomene* is more like mimic and *H. erato* more like model (Mallet and Turner 1998). This asymmetry in comimicking species would produce an additional selective force that is characteristic of Batesian mimicry interaction. How much this additional factor affect the speed of cline movement and the maintenance of spatial mosaic is still open to question.

To conclude, we have shown that the similarity between comimicking pair of morphs is not in general effective in slowing down the wave speed of the mimetic morph boundary, in a stochastic cellular automaton model (lattice model) of two species Müllerian mimicry. On the other hand, spatial heterogeneity in migration rates can stably trap the boundary of mimetic morph distribution near a steep trough of migration rate, even when the process is largely perturbed by demographic noise. Though the spatial mosaic structure in Müllerian mimicry rings in itself can be formed by frequency-dependent selection favoring a commoner morph, more attention should be paid for the role of spatial heterogeneity in the environment to account for its stable maintenance.

## **Acknowledgement**

We thank S. Tohya for his helpful comments, and three reviewers for discussion and comments. A.S. acknowledges the support from the Japanese Society for the Promotion of Sciences, Japanese Ministry of Education and Sciences.

## Appendix A

We define  $p_d(t)$  as the probability that, at time  $t$ ,  $A$ -front runner in species 1 is  $d$  step ahead of the  $a$ -front-runner in species 2, which then obey a birth-death process:

$$\dot{p}_d = \mu_{d+1}p_{d+1} + \lambda_{d-1}p_{d-1} - \mu_d p_d - \lambda_d p_d, \quad (d = 0, \pm 1, \pm 2, \dots) \quad (\text{A.1})$$

where  $\lambda_d$  is the transition rate from  $d$  to  $d+1$ , and  $\mu_d$  is the transition rate from  $d$  to  $d-1$ , which will be specified below. There are two ways by which the distance change from  $d$  to  $d+1$  -- one is that the  $A$  front-runner moves a step forward in species 1, and the other is that the  $a$  front runner moves a step backward in species 2. This and similar consideration for the transition from  $d$  to  $d-1$  yield the transition rates  $\lambda_d$ 's and  $\mu_d$ 's:

$$\lambda_d = \mu_{-d} = u_0 + u_1 \begin{cases} [\varphi_A(2+3\sigma) + \varphi_B(2+3\sigma)]/2, & (d \geq 1) \\ [\varphi_A(2+2\sigma) + \varphi_B(2+2\sigma)]/2, & (d = 0) \\ [\varphi_A(2+\sigma) + \varphi_B(2+\sigma)]/2, & (d = -1) \\ [\varphi_A(2) + \varphi_B(2)]/2, & (d \leq -2) \end{cases} \quad (\text{A.2})$$

The stationary probability density  $\hat{p}_d$  must satisfy

$$\lambda_d \hat{p}_d = \mu_{d+1} \hat{p}_{d+1} \quad (\text{A.3})$$

From (A1) and (A3), we see that  $\hat{p}_d$  is symmetric with respect to  $d$  around 0

$$\hat{p}_d = \hat{p}_{-d}. \quad (\text{A.4})$$

Thus we have

$$\sum \hat{p}_d = \dots + \hat{p}_{-d} + \dots + \hat{p}_{-2} + \hat{p}_{-1} + \hat{p}_0 + \hat{p}_1 + \hat{p}_2 + \dots + \hat{p}_d + \dots$$

$$\begin{aligned}
&= \hat{p}_0 + 2 \sum_{k=1}^{\infty} \hat{p}_k \\
&= \hat{p}_0 + 2(\theta_1 \hat{p}_0 + \theta_2 \theta_1 \hat{p}_0 + \theta_2^2 \theta_1 \hat{p}_0 + \theta_2^3 \theta_1 \hat{p}_0 + \dots) \\
&= \hat{p}_0 + 2\theta_1 \hat{p}_0 \sum_{k=0}^{\infty} \theta_2^k \\
&= \hat{p}_0 + 2\theta_1 \hat{p}_0 \frac{1}{1-\theta_2} = 1
\end{aligned} \tag{A.5}$$

where  $\theta_1 = \lambda_0 / \mu_1$  and  $\theta_2 = \lambda_1 / \mu_2$ . It is clear from (A.3) that  $\theta_2 < 1$  as long as  $\sigma > 0$ .

From this,  $\hat{p}_0$  is obtained as

$$\hat{p}_0 = \frac{1}{1 + 2\theta_1(1-\theta_2)^{-1}}. \tag{A.6}$$

From (A.3), (A.4) and (A.6), the stationary distribution (7) in the text is obtained

## Appendix B

We here derive the stationary distribution for the position of the front runner, for the case where migration rate varies spatially. From the master equation (14) describing the change in  $q_x(t)$ , the probability that the front runner is in the site  $x$  at time  $t$ , we see that the stationary distribution  $\hat{q}_x$  of the process, if it exists, must satisfy

$$\lambda_x \hat{q}_x = \mu_{x+1} \hat{q}_{x+1}. \quad (\text{B.1})$$

Using the transition rate (15), we then have

$$\begin{aligned} \hat{q}_{x+1} &= \frac{\lambda_x}{\mu_{x+1}} \hat{q}_x \\ &= \frac{m_x}{m_{x+2}} \left( \frac{d_B(2)}{d_A(2)} \right) \hat{q}_x \end{aligned} \quad (\text{B.2})$$

and hence

$$\hat{q}_x = \frac{m_1 m_0}{m_{x+1} m_x} \left( \frac{d_B(2)}{d_A(2)} \right)^x \hat{q}_0. \quad (\text{B.3})$$

From this and  $\sum_{x=-\infty}^{\infty} \hat{q}_x = 1$ , we can obtain  $\hat{q}_0$  as

$$\hat{q}_0 = \left( m_1 m_0 \sum \frac{1}{m_{y+1} m_y} \left( \frac{d_B(2)}{d_A(2)} \right)^y \right)^{-1}. \quad (\text{B.4})$$

where sum is over all  $y$ . Hence (B3) becomes

$$\hat{q}_x = \frac{1}{m_{x+1} m_x} \left( \frac{d_B(2)}{d_A(2)} \right)^x \left( \sum \frac{1}{m_{y+1} m_y} \left( \frac{d_B(2)}{d_A(2)} \right)^y \right)^{-1}, \quad (\text{B.5})$$

which gives the stationary distribution (16) in the text.

## Literature Cited

- Barton, N. 1979. The dynamics of hybrid zones. *Heredity* 43:341-359.
- Barton, N., and G. M. Hewitt. 1989. Adaptation, speciation and hybrid zones. *Nature* 341:497-503.
- Bazykin, A. D. 1969. Hypothetical mechanism of speciation. *Evolution* 23:685-687.
- Blum, M.J. 2002. Rapid movement of a *Heliconius* hybrid zone: evidence for phase III of Wright's shifting balance theory? *Evolution* 56, 1992-1998.
- Brown, K. S., and W. W. Benson. 1974. Adaptive polymorphism associated with multiple Mullerian mimicry in *Heliconius numata* (Lepidoptera: Nymphalidae). *Biotropica* 6:205-228.
- Dasmahapatra, K.K., Blum, M., Aiello, A., Hackwell, S., Davies, N., Bermingham, E.P., and Mallet, J. 2002. Inferences from a rapidly moving hybrid zone. *Evolution* 56, 741-753.
- Ellner, S., A. Sasaki, Y. Haraguchi, and H. Matsuda. 1998. Speed of invasion in lattice population models: pair-edge approximation. *J. Math. Biol.* 36:469-484.
- Gilbert, L. 1983. Coevolution and Mimicry. Pp. 263-281 in D. J. Futuyma and M. Slatkin, eds. *Coevolution*. Sinauer Associates Inc., Sunderland.
- Joron, M., and J. L. B. Mallet. 1998. Diversity in mimicry: paradox or paradigm? *TREE* 13:461-466.
- Mallet, J., N. Barton, G. M. Lamas, J. C. Santisteban, M. M. Muedas, and H. Eeley. 1990. Estimate of selection and gene flow from measures of cline width and linkage disequilibrium in *Heliconius* hybrid zones. *Genetics* 124:921-936.
- Mallet, J. 1993. Speciation, raiation, and color pattern evolution in *Heliconius* butterflies: evidence from hybrid zones. *In: Hybrid Zones and the Evolutionary Process*. (Ed: Harrison, RG) Oxford University Press, New York, 226-260
- Mallet, J., and L. E. J. Gilbert. 1995. Why are there so many mimicry rings? -- Correlations between habitat, behaviour and mimicry in *Heliconius* butterflies. *Biological Journal of the Linnean Society* 55:159-180.

- Mallet, J. L. B., and J. R. G. Turner. 1998. Biotic drift or the shifting balance -- did forest islands drive the diversity of warningly coloured butterflies? Pp. 262-280 in P. R. Grant, ed. *Evolution on Islands*. Oxford University Press, Oxford.
- Mallet, J. and Joron, M. 1999. The evolution of diversity in warning colour and mimicry: polymorphisms, shifting balance, and speciation. *Ann. Rev. Ecol. Syst.* 30, 201-233.
- Mallet, J. 2001, Causes and consequences of a lack of coevolution in Müllerian mimicry., *Evol. Ecol.* 13(7/8), 777-806.
- Kawasaki, K., Fugo, T., Caswell, H. and Shigesada, N. 2006. How does stochasticity in colonization accelerate the speed of invasion in a cellular automaton model? *Ecological Research*, **21**, 334-345
- Sasaki, A., I. Kawaguchi, and A. Yoshimori. 2002, Spatial mosaic and interfacial dynamics in Müllerian mimicry system. *Theor. Pop. Biol.* 61, 49-71
- Turner, J. R. G. 1981. Adaptation and evolution in *Heliconius*: A defense of Neo Darwinism. *Ann. Rev. Ecol. Syst.* 12:99-121.
- Turner, J. R. G. 1984. Mimicry: The palatability spectrum and its consequences. Pp. 141-161 in R. I. Vane-Wright and P. R. Ackery, eds. *The Biology of Butterflies*. Academic Press, London.

## Figure Legend

**Figure 1.** A typical spatial distributions of mimetic morphs in each comimicking species on a linear lattice. In each location  $x$ , there are two sites occupied respectively by each species. Each site for species 1 is occupied by an individual with either warning coloration A (filled circle) or B (open circle), and each site for species 2 by an individual with a (filled box) or b (open box). Warning coloration A and a are a comimicking pair, and B and b are another comimicking pair. The location where A and B meets defines the mimetic morph boundary for species 1, and the location where a and b meets defines that for species 2. Each mimetic morph boundary may move one step right or left by the death of individual at the edge and colonization by adjacent individual of the other morph. The number of the identical morph of the same species and the comimicking morph of the other species in the neighborhood (e.g. sites enclosed by the rectangle for and individual at location  $x$ ) determines the mortality of an individual.

**Figure 2.** The effect of the degree  $\sigma$  of similarity between comimicking pair of morphs on the joint speed at which the advantageous morph propagates in each species. Solid line shows the predicted wave speed obtained from equation (9), and dots show the speeds observed in Monte Carlo simulations. The speed decreases as the similarity  $\sigma$  increases toward 1.  $\delta = \log 7$ ,  $\alpha_A = 2.0$ ,  $\alpha_B = 2.5$ ,  $u_0 = 0$ ,  $u_1 = 1$ .

**Figure 3.** The joint speed of the propagation of advantageous comimicking pair of morphs as a function of similarity  $\sigma$  between them, for several values of inflection density  $\alpha_B$ . The speed monotonically decreases with  $\sigma$  if  $\alpha_B = 2$  (thick line); has a hump

at intermediate  $\sigma$  if  $\alpha_B = 3$  (medium thick line); and monotonically increases with  $\sigma$  if  $\alpha_B = 5$  (thin line). These results indicate that increasing  $\sigma$  does not always decrease the speed of cline movement. If a linear density dependence in predation rates is assumed:  $d_A(N) = u_0 + a - u_1\delta(N - \alpha_A)$  and  $d_B(N) = u_0 + a - u_1\delta(N - \alpha_B)$ , the speed is independent of the similarity  $\sigma$  (broken line). Parameters are  $\delta = \log 7$ ,  $\beta = 0.1$ ,  $u_0 = 0$ , and  $u_1 = 1$ . For the case of linear density dependence,  $a = 10$  and  $\alpha_B = 5$  are used.

**Figure 4.** The variance in the distance between the mimetic morph boundary in species 1 and that in species 2, plotted in logarithmic scale as a function of two parameters  $\theta_1$  and  $\theta_2$  of the stationary density  $\hat{p}_d$ . (a) The variance in  $d$  most sensitively increases as  $\theta_2$  approaches 1. (b) The dependence of  $\theta_2$  on  $\delta$  and  $\sigma$ .  $\theta_2$  approaches to 1 when  $\delta$  is close to 0 or  $\sigma$  is sufficiently smaller than  $\{2(\alpha_B - 2) + \beta\}/2$ , which is the inflection point of  $\theta_2$  as a function of  $\delta$ . Parameters are  $\alpha_B = 3$ ,  $\beta = 0.1$ ,  $u_0 = 0$ , and  $u_1 = 1$

**Figure 5.** Simulation result with a spatial heterogeneity of migration rates in single species system. The migration rate  $m(x)$  at the position  $x$  is assumed to have a valley centered at  $x=0$ :  $m(x) = \exp(ax^2)$  for  $0 \leq |x| < 10$ , where  $a=0.05$ . Outside this range ( $|x| > 10$ ), the migration rate stays the same as the value at  $x=10$ . (a) Time series of the positions observed in a Monte Carlo simulation. (b) The stationary distribution for the position  $x$ . The long term average distribution for the positions of boundary observed in Monte Carlo simulation (filled circle) is compared with the predicted distribution (solid line). Both figure show how the mimetic morph boundary is trapped around  $x=0$  at which the migration rate is minimum. Parameters are  $\delta = \log 7$ ,  $\alpha_B = 0.5$ ,  $\beta = 0.1$ ,  $u_0 = 0$ , and  $u_1 = 1$ .

Fig 1

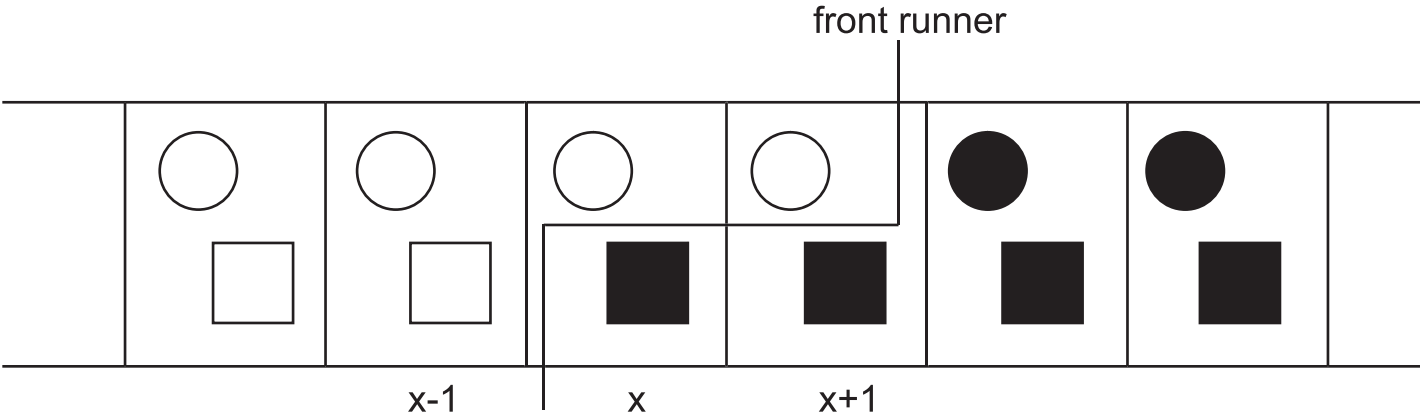


Fig 2

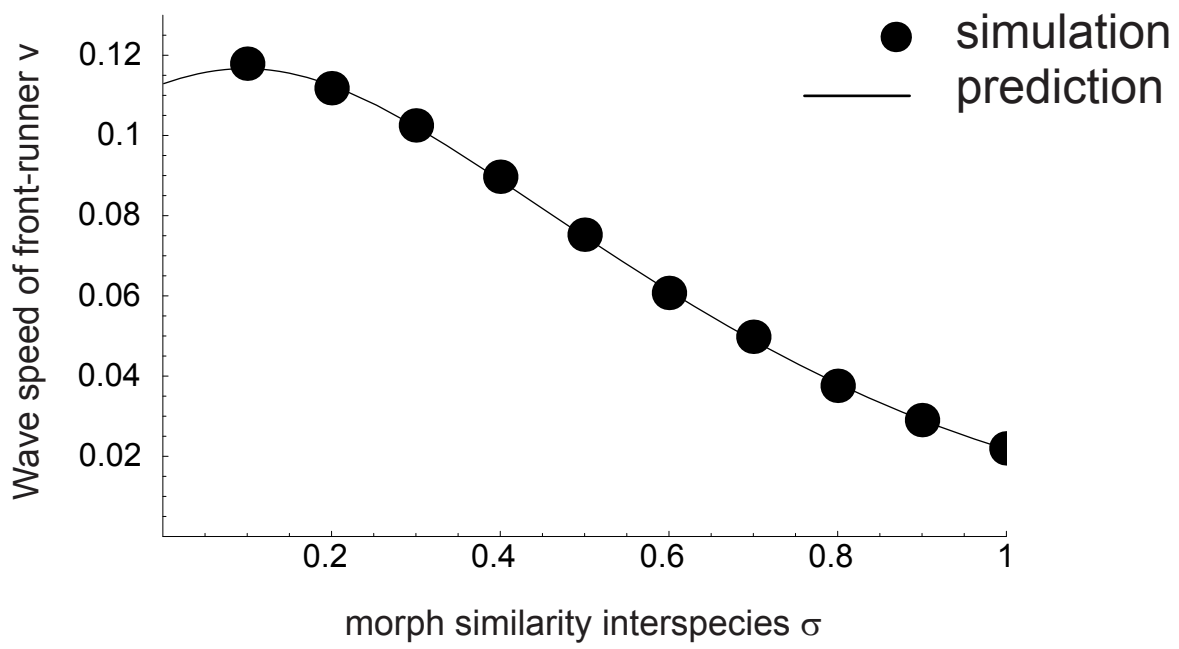


Fig 3

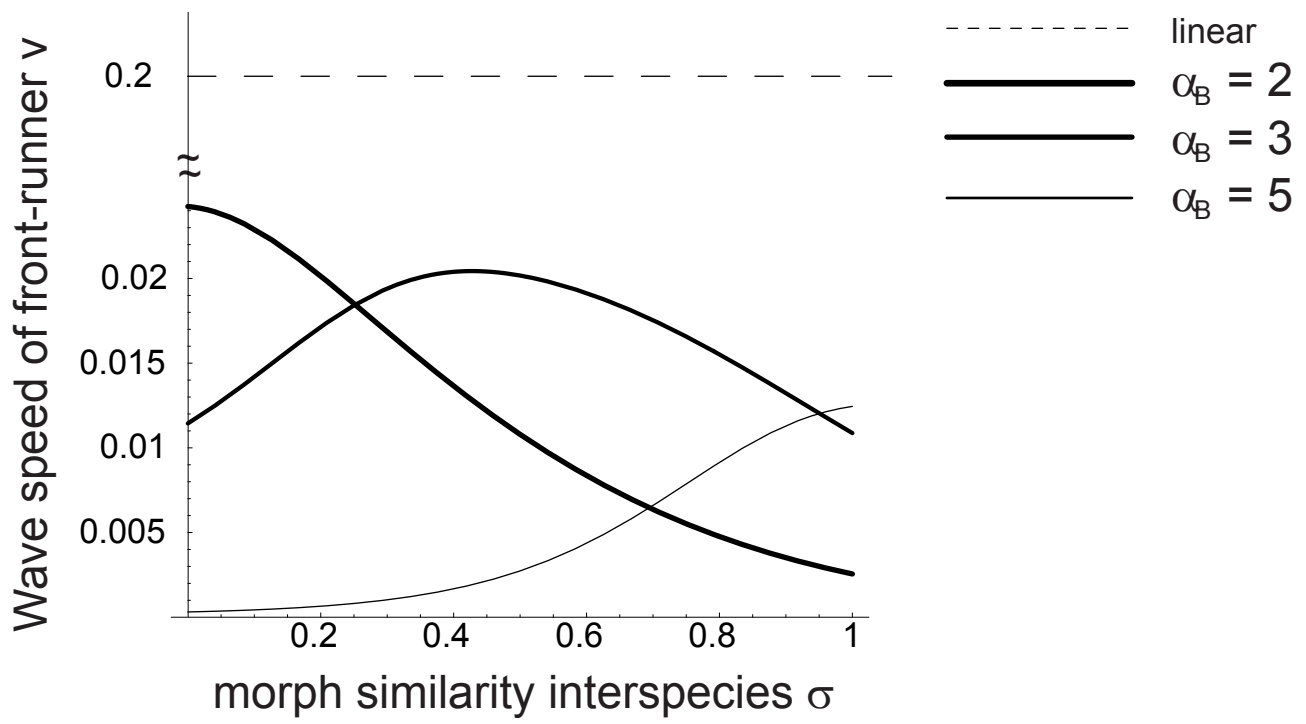
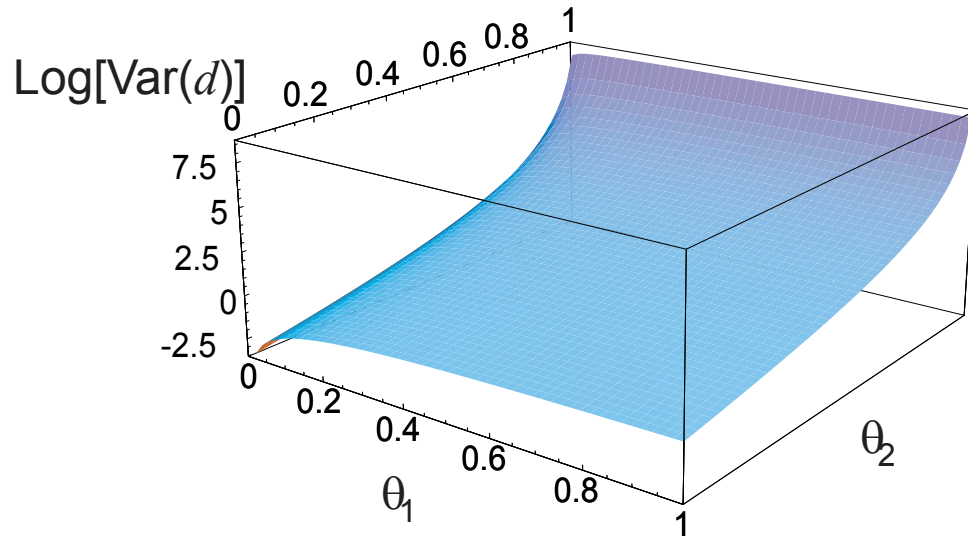
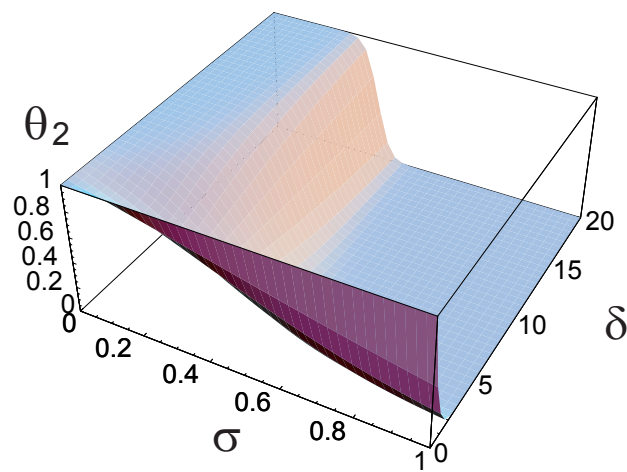


Fig 4

(a)

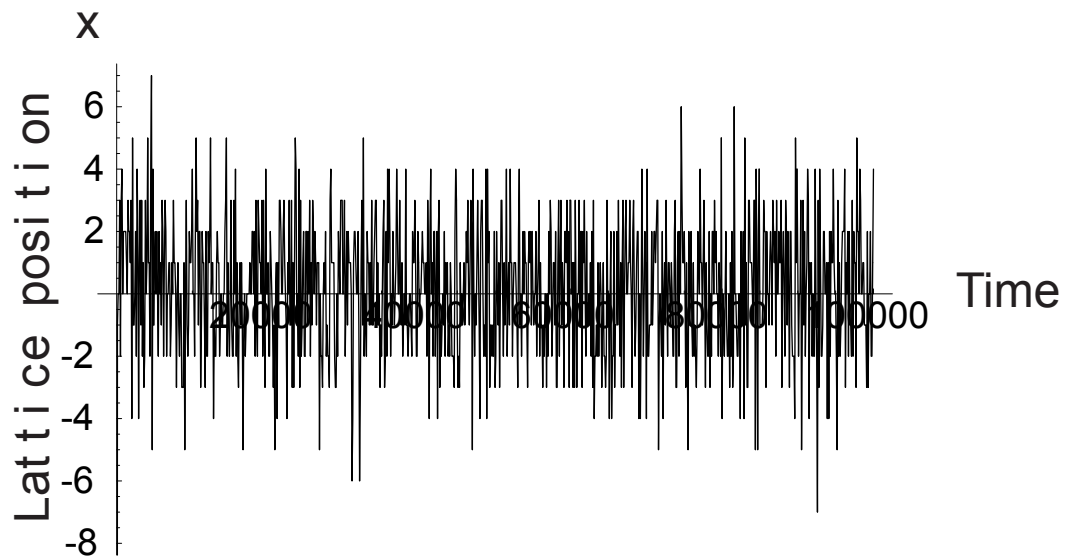


(b)



$$\alpha_B = 3$$

(a)



(b)

